



Mechanistic, energetic and structural studies of single-walled carbon nanotubes functionalized with penicillamine

HOSEIN SHAKI¹, ALI MORSALI^{2*}, HEIDAR RAISSI³, MOHAMMAD HAKIMI¹
and S. ALI BEYRAMABADI²

¹Department of Chemistry, Payame Noor University, P. O. Box 19395-3697, Tehran, Iran,

²Department of Chemistry, & Research Center for Animal Development Applied Biology,
Mashhad Branch, Islamic Azad University, Mashhad 917568, Iran and ³Department of
Chemistry, University of Birjand, Birjand, Iran

(Received 18 February, revised 29 May, accepted 6 June 2017)

Abstract: Using the density functional theory, the possible non-covalent interactions and six mechanisms of covalent functionalization of the drug penicillamine with functionalized carbon nanotubes (CNT) were investigated. Quantum molecular descriptors of the non-covalent configurations were studied. It was determined that binding of the drug penicillamine with functionalized CNT is thermodynamically viable. COOH functionalized CNT (NTCOOH) has more binding energy than COCl functionalized CNT (NTCOCl) and could act as a favorable system for penicillamine drug delivery within biological and chemical systems (non-covalent). NTCOOH and NTCOCl can bond to the NH₂, OH and SH groups of penicillamine through OH (COOH mechanism) and Cl (COCl mechanism) groups, respectively. The activation energies, activation enthalpies and activation Gibbs energies of six pathways were calculated and compared with each other. The activation parameters related to the COOH mechanism are higher than those related to the COCl mechanism and therefore, the COCl mechanism is suitable for covalent functionalization. These results could be generalized to other similar drugs.

Keywords: density functional theory; quantum molecular descriptors; covalent and non-covalent functionalization; reaction mechanisms.

INTRODUCTION

Although many efforts have been made to overcome cancer through chemotherapy, the old strategies and approaches induce many side effects, such as vomiting, hair loss, cardio-toxicity and breathing troubles, in patients. The higher the dose of anti-cancer drugs prescribed and used, the higher the increase of toxicity in the tissues and immune system of the body.^{1,2}

*Corresponding author. E-mails: almorsali@yahoo.com, morsali@mshdiau.ac.ir
<https://doi.org/10.2298/JSC170218072S>

Carbon nanotubes (CNTs) show unique mechanical, photonic, electronic, and chemical properties,^{3–5} resulting in their use in biological and pharmaceutical research.^{6–8} In spite of issues such as low solubility and that they will not be easily discharged from the body, there has been increasing interest in CNTs as drug delivery systems in recent years.^{9–12} In addition, the interaction of organic and inorganic molecules with carbon nanotubes has been extensively studied.^{13–17}

Due to their high drug loading capacities and good cell penetration qualities,¹⁸ CNTs could perform better than systems such as polymers, dendrimers, and liposomes normally used for drug delivery.^{19,20}

The use of CNTs for drug delivery to cancerous tissues confirmed that the side effects of the drug were decreased in numerous cases.^{21,22} Covalent and non-covalent (hydrogen bonds and van der Waals interactions) functionalization play a principle role in the drug delivery systems.

Penicillamine is used in the genetic disorder of copper metabolism (Wilson's disease) and rheumatoid arthritis.^{23,24} Furthermore, it has been used as a chemopreventive agent. Recent investigations showed cell growth inhibition in several different types of cancer cells.^{25,26}

Quantum calculations could be of great assistance in the design and analysis of drug delivery systems. The granting of the Nobel Prize for Chemistry in 2016 for the design and manufacture of molecular machines capable of employment in drug deliverance as well confirms the above statement.^{27–29}

In this study, quantum calculations were used for the analysis of the more stable structures and the mechanism of functionalization of the drug penicillamine to CNTs. Such calculations could inspire researchers in the manufacture of new drug delivery systems.^{6,30} In spite of different theoretical studies on CNTs, hitherto, few studies have considered the mechanism of functionalization.

COMPUTATIONAL DETAILS

The UB3LYP hybrid density functional level,^{31–33} and the 6-31G(d,p)basis sets in the Gaussian 09 package (rev. A.02)³⁴ were used for the optimization of all degrees of freedom for all geometries in the solution phase. The solvent plays a key role in chemical systems explicitly^{35–43} or implicitly. The polarized continuum model (PCM)^{44,45} was used for the consideration of the implicit effects of the solvent. In the PCM method, the molecular cavity is made up of the union of interlocking atomic spheres.

Unrestricted methods (U in UB3LYP) are needed for chemical species with unpaired electrons such as configurations with odd numbers of electrons (NTCOOH and NTCOCl) and reactions such as bond dissociation (covalent functionalization).⁴⁶

The calculations were performed on penicillamine, COOH (in water) and COCl (in DMF) functionalized armchair (5,5) single-walled carbon nanotubes (SWCNT) comprising 114 atoms (10 Å) with the ends terminated by hydrogen atoms. In spite of the high computational cost, approximation methods, such as ONIOM,⁴⁷ were not used.

Quantum molecular descriptors such as hardness and electrophilicity index could be used to describe chemical reactivity and stability.

The global hardness (η), indicating the resistance of one molecule against a change in its electronic structure, is given by Eq. (1):

$$\eta = (I - A) / 2 \quad (1)$$

where $I = -E_{\text{HOMO}}$ and $A = -E_{\text{LUMO}}$ are the ionization potential and the electron affinity of the molecule, respectively. A decrease in η causes a decrease in reactivity and an increase in stability.

Parr defined the electrophilicity index (ω) as follows⁴⁸:

$$\omega = \mu^2 / 2\eta \quad (2)$$

RESULTS AND DISCUSSION

Penicillamine (PCA) is a non-planar molecule with NH_2 , OH and SH groups, as presented in Fig. 1. The optimized geometries of PCA, COOH (NTCOOH) and COCl (NTCOCl) functionalized SWCNT in solution phase are shown in Fig. 1. Use of the functionalized CNTs as well as the drugs having NH_2 , OH and SH groups causes an increase in the solubility of carbon nanotubes.

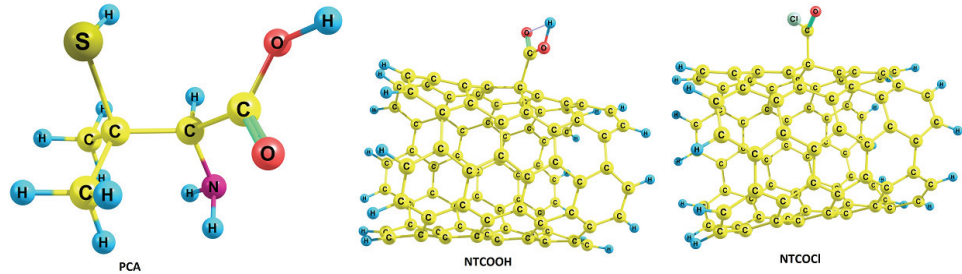


Fig. 1. Optimized structures of PCA, NTCOOH and NTCOCl.

The interaction between PCA and NTCOOH or NTCOCl through NH_2 , OH and SH groups, forms hydrogen bonds. These six reactants (R) are shown in Figs. 2 and 3, namely, NTCOOH/PCA1–3R and NTCOCl/PCA1–3R, respectively, (see the Supplementary material to this paper for the Cartesian coordinates of the calculated structures).

The binding energies (ΔE) of PCA to NTCOOH (in water) and NTCOCl (in DMF) were calculated using the following equation and are presented in Table I:

$$\Delta E = E_{\text{NTCOOH(NTCOCl)/PCA1-3R}} - (E_{\text{NTCOOH(NTCOCl)}} + E_{\text{PCA}}) \quad (3)$$

The calculated binding energies of the six configurations in Table I are negative in the solution phase indicating that PCA is stabilized by the NTCOOH and NTCOCl surfaces. Among the six configurations, those related to NTCOOH are more stable than are those of the NTCOCl configurations. Among the three configurations of NTCOOH/PCA1–3R, the first one has a more negative energy, denoting a stronger interaction (from the NH_2 group).

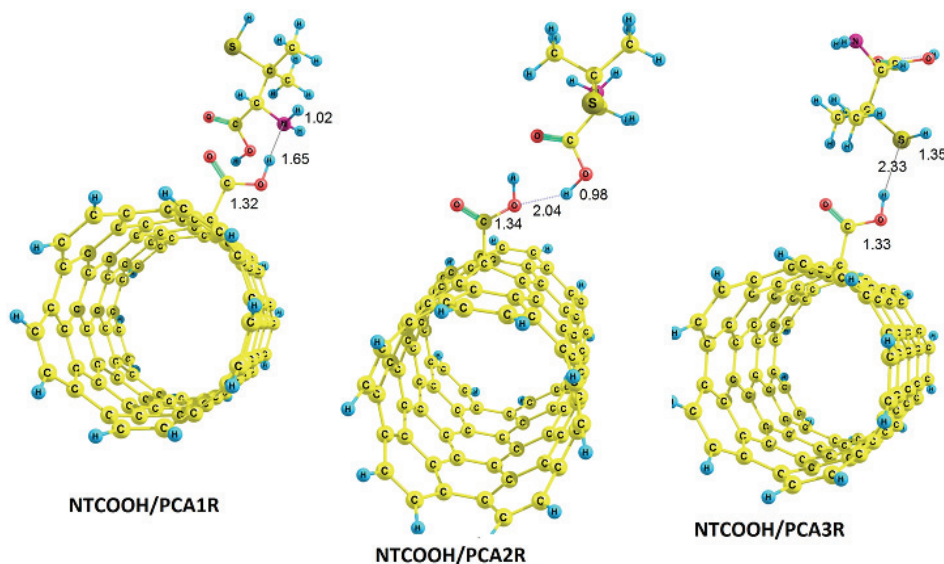


Fig. 2. Optimized structures of reactants NTCOOH/PCA1–3R.

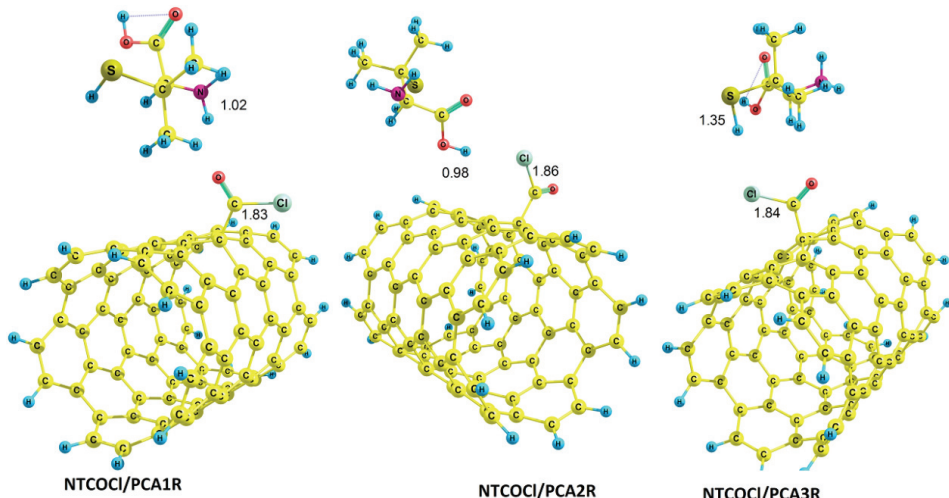


Fig. 3. Optimized structures of reactants NTCOCl/PCA1–3R.

To evaluate the quantities obtained from the B3LYP functional, the binding energy of NTCOOH/PCA1R was calculated using the UM062X functional, which is suitable for non-covalent interactions.⁴⁹ The binding energy is equal to -47.31 kJ mol⁻¹ (See the Supplementary material), being compatible with the quantity obtained from the B3LYP functional.

TABLE I. Quantum molecular descriptors (eV) and binding energies (kJ mol⁻¹) for the optimized geometries of PCA, NTCOOH (H₂O), NTCOCl (DMF), NTCOOH/PCA1–3R (H₂O) and NTCOCl/PCA1–3R (DMF).

Species	<i>E</i> _{HOMO}	<i>E</i> _{LUMO}	<i>E</i> _g	<i>η</i>	<i>ω</i>	<i>ΔE</i>
PCA (H ₂ O)	-6.47	0.0136	6.48	3.24	1.61	—
PCA (DMF)	-6.46	0.0180	6.48	3.24	1.60	—
NTCOOH	-4.04	-2.74	1.30	0.65	8.86	—
NTCOCl	-4.07	-2.82	1.26	0.63	9.46	—
NTCOOH/PCA1R	-4.02	-2.71	1.31	0.66	8.63	-41.00
NTCOOH/PCA2R	-4.04	-2.74	1.30	0.65	8.82	-28.17
NTCOOH/PCA3R	-3.91	-2.73	1.18	0.59	9.36	-18.59
NTCOCl/ PCA1R	-4.08	-2.82	1.26	0.63	9.48	-5.70
NTCOCl/ PCA2R	-4.09	-2.84	1.25	0.62	9.59	-4.68
NTCOCl/ PCA3R	-4.08	-2.82	1.26	0.63	9.46	-3.80

Generally, for non-covalent interactions, a comparison between COOH and COCl functionalized single wall carbon nanotubes shows that using the former is more suitable due to the stronger interaction between PCA and SWCNT.

Table I presents the quantum molecular descriptors for PCA, NTCOOH (H₂O), NTCOCl (DMF), NTCOOH/PCA1–3R(H₂O) and NTCOCl/PCA1–3R (DMF). In this table, *E*_g (the gap in energy between LUMO and HOMO) is also given. *E*_g notably determines a more stable system.

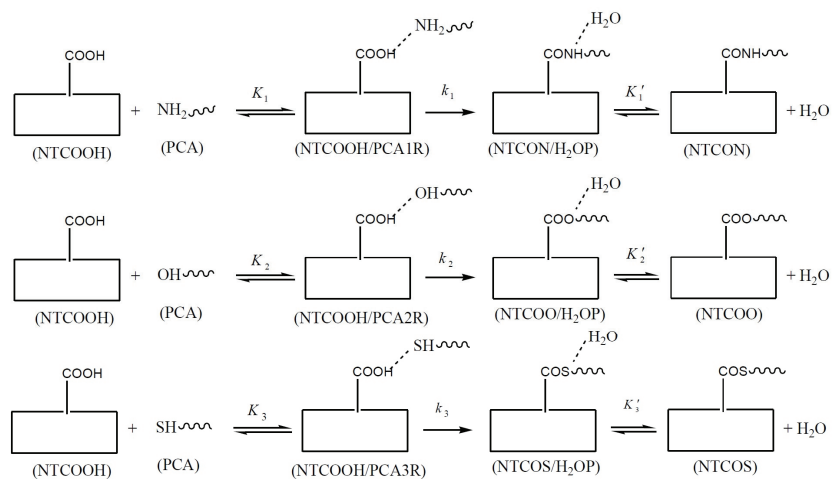
According to the data in Table I, the *η* and *E*_g values related to the PCA drug are higher than those of NTCOOH/PCA1–3R and NTCOCl/PCA1–3R, showing the stability of PCA decreases in the presence of COOH (COCl) functionalized SWCNT and its reactivity increases. The *ω* value of PCA increases in the presence of COOH (COCl) functionalized SWCNT, showing that PCA acts as an electron acceptor.

For the covalent functionalization, NH₂, OH and SH groups attack the carbon atom of COOH or COCl to transfer their protons to the OH (Cl) group. The six possible mechanisms for NTCOOH(Cl)/PCA1–3R were studied.

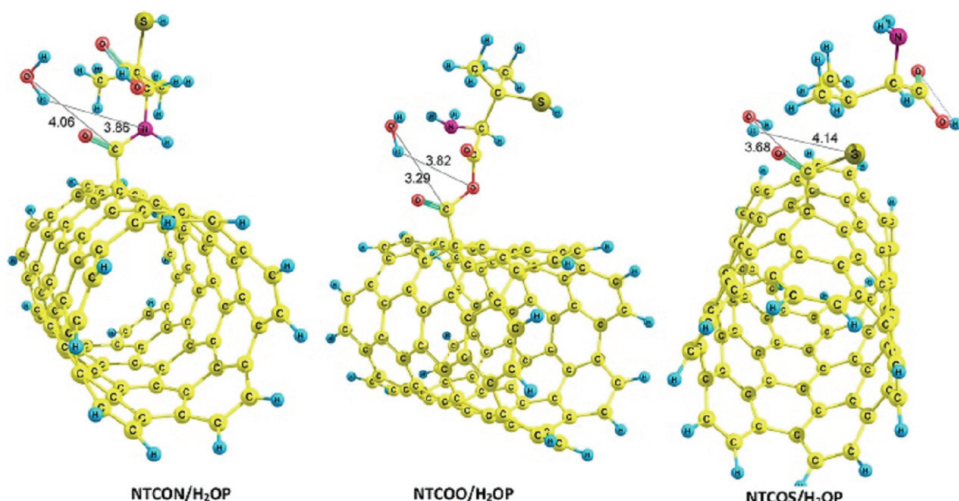
The mechanism for the formation of covalent bond between PCA and NTCOOH (COOH mechanism) is shown in Scheme 1, where *k*₁ (*k*₂, *k*₃) is the rate constant and *K*₁ and *K*_{1'} (*K*₂, *K*_{2'}, *K*₃ and *K*_{3'}) are equilibrium constants. In this mechanism, NTCOOH/PCA1R(2R,3R) is converted into the product NTCON (O,S) by losing H₂O.

According to Scheme 1, in the COOH mechanism, the OH from NTCOOH is substituted by NH (O,S) from PCA to give the products NTCON (O,S). The optimized structure of the products NTCON(O,S)/H₂OP are shown in Fig. 4.

Using the reactant NTCOOH/PCA1R and the product NTCON/H₂OP, the transition state of the *k*₁ step was optimized, which is called TS_{*k*₁} (Fig. 5). The calculated bond lengths are shown in Figs. 2, 4 and 5.



Scheme 1. COOH mechanism of covalent functionalization.

Fig. 4. Optimized structures of the products NTCOON(O,S)/H₂OP.

The relative energies for the optimized structures in all pathways, given in Table II, were calculated by considering the electronic plus zero point energy (E), enthalpy (H) and Gibbs free energy (G) of the reactants (NTCOOH+PCA) equal to zero (see the Supplementary material for the absolute energies). The activation energy (E_a), activation enthalpy (ΔH^\ddagger) and activation Gibbs free energy (ΔG^\ddagger) for the k_1 step are 218.83 kJ mol⁻¹, 217.00 kJ mol⁻¹ and 229.26 kJ mol⁻¹, respectively (Table II). The total rate constant for the overall reaction (COOH/NH pathway) is equal to $k_1 \times K_1$, and hence the total activation energy is:

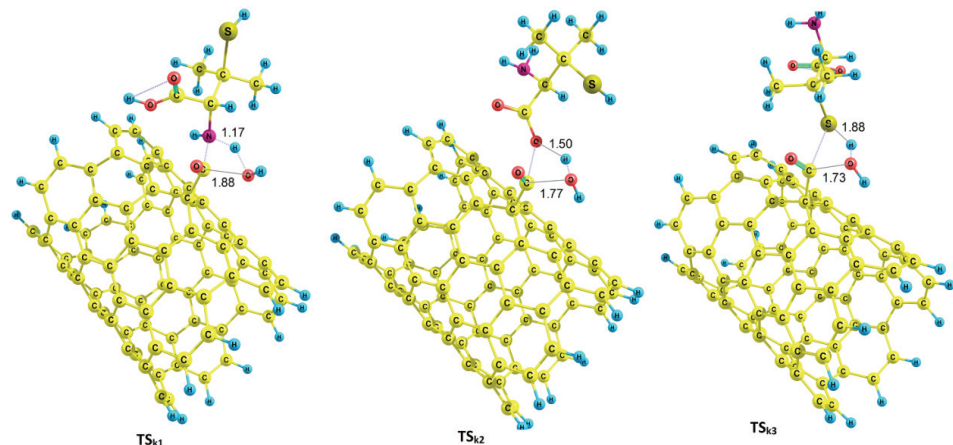


Fig. 5. Optimized structures of TS_{k1} , TS_{k2} and TS_{k3} .

$E_a(\text{COOH})(\text{NH}) = E_a(k_1 \text{ step} + \Delta E(K_1 \text{ step})) = 177.83 \text{ kJ mol}^{-1}$, the total activation enthalpy change is: $\Delta H^\ddagger(\text{COOH})(\text{NH}) = \Delta H^\ddagger(k_1 \text{ step} + \Delta H(K_1 \text{ step})) = 179.66 \text{ kJ mol}^{-1}$ and the total activation Gibbs energy change is: $\Delta G^\ddagger(\text{COOH})(\text{NH}) = \Delta G^\ddagger(k_1 \text{ step} + \Delta G(K_1 \text{ step})) = 231.90 \text{ kJ mol}^{-1}$ for the COOH/PCA1 mechanism (Table II).

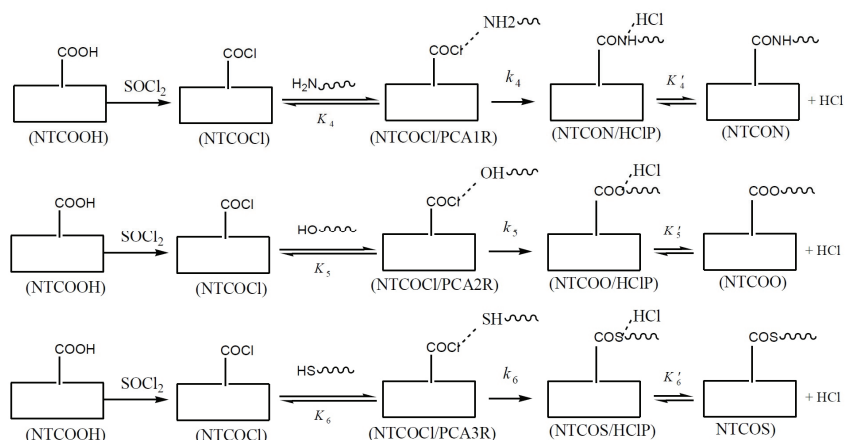
Similar to the k_1 step, using NTCOOH/PCA2R (NTCOOH/PCA3R) and NTCOO/H₂OP (NTCOS/H₂OP), the transition state of the k_2 (k_3) step (Fig. 5) was obtained, which is called TS_{k1} (TS_{k2}). The E_a , ΔH^\ddagger and ΔG^\ddagger values for the k_2 (k_3) step are 206.12, 203.16 and 214.54 kJ mol⁻¹ (216.63, 215.10 and 226.43 kJ mol⁻¹), respectively (Table II). Using equations similar to the ones given for the COOH/PCA1 mechanism, the total activation energy, the total activation enthalpy change and the total activation Gibbs energy change for the COOH/PCA2 (COOH/PCA3) mechanism are 177.95, 181.70 and 228.35 kJ mol⁻¹ (198.04, 201.56 and 246.74 kJ mol⁻¹), respectively (Table II). At room temperature, the energy barriers related to COOH mechanism are too high for it to occur.

The other reactions for the covalent functionalization of PCA onto COCl functionalized carbon nanotubes are shown in Scheme 2 (COCl mechanism).⁵⁰ In these reactions, NTCOOH was first converted into the acyl chloride using SOCl₂ (NTCOCl). PCA then reacts with NTCOCl to form a covalent bond. NTCOCl is again converted to NTCOOH in the presence of water. Therefore, this process should take place in a solvent such as DMF.⁵⁰ Experimentally, it could be solved in water after replacement of Cl with the drug. Water solvent was considered for NTCOOH, because water is the main solvent in the human body.

COCl mechanism begins with the attack of NH₂, OH and SH of PCA on Cl in the NTCOCl to form the products NTCON/HClP, NTCOO/HClP and NTCOS/HClP, respectively (Fig. 6).

TABLE II. Relative energies for the different species in the COOH and COCl mechanisms. E , H and G are the electronic plus zero point energy, enthalpy and Gibbs free energy, respectively

Species	E / kJ mol ⁻¹	H / kJ mol ⁻¹	G / kJ mol ⁻¹
In water	COOH mechanism		
NTCOOH+PCA	0.00	0.00	0.00
NTCOOH/PCA1R	-41.00	-37.34	2.64
TS _{k1}	177.83	179.66	231.90
NTCON/H2OP	-28.61	-22.97	20.17
NTCOOH/PCA2R	-28.17	-23.46	13.81
TS _{k2}	177.95	181.70	228.35
NTCOO/H2OP	38.10	45.04	80.66
NTCOOH/PCA3R	-18.59	-13.54	20.31
TS _{k3}	198.04	201.56	246.74
NTCOS/H2OP	29.59	37.30	70.26
In DMF	COCl mechanism		
NTCOCI+PCA	0.00	0.00	0.00
NTCOCI/PCA1R	-5.70	0.65	24.97
TS _{k4}	21.79	23.42	75.01
NTCON/HClP	-95.07	-90.92	-54.15
NTCOCI/PCA2R	-4.68	1.41	30.20
TS _{k5}	84.32	88.31	129.12
NTCOO/HClP	-21.08	-15.41	18.71
NTCOCI/PCA3R	-3.80	2.44	29.16
TS _{k6}	75.05	74.88	128.82
NTCOS/HClP	-26.54	-23.03	15.76



Scheme 2. The COCl mechanism of covalent functionalization.

Using NTCOCI/PCA1R and NTCON/HClP, a transition state is optimized, which is called TS_{k4} (Fig. 7). The calculated bond lengths are presented in Figs. 3, 6 and 7. The values of E_a , ΔH^\ddagger and ΔG^\ddagger for k_4 step are 27.49, 24.07 and 50.22

kJ mol^{-1} , respectively (Table II). The total activation energy, the total activation enthalpy change and the total activation Gibbs energy change for the $\text{COCl}/\text{PCA1}$ mechanism are 21.79, 23.42 and 75.01 kJ mol^{-1} , respectively (Table II).

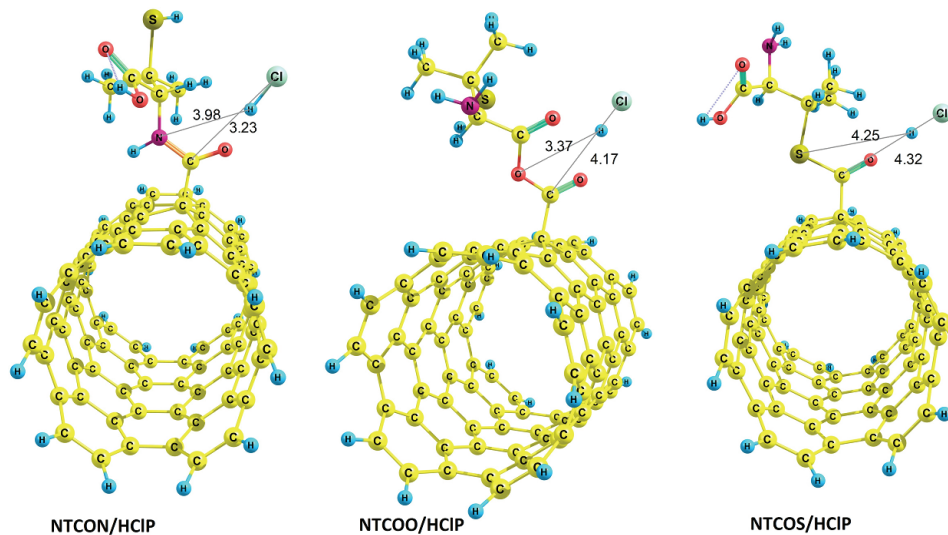


Fig. 6. Optimized structures of the products $\text{NTCO(O,S)}/\text{HClP}$.

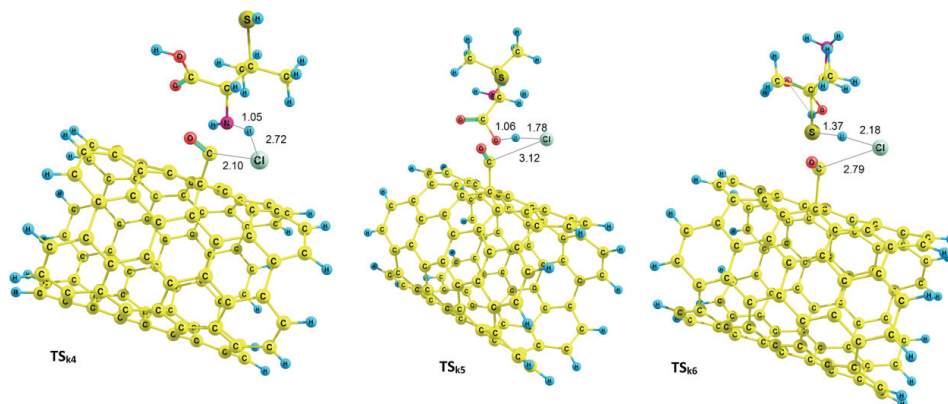


Fig. 7. Optimized structures of TS_{k4} , TS_{k5} and TS_{k6} .

Using the reactants $\text{NTCOCl}/\text{PCA2R}$ and $\text{NTCOCl}/\text{PCA3R}$ and the products NTCOO/HClP and NTCOS/HClP , the transition states of the k_5 and k_6 steps were obtained, which are called TS_{k5} and TS_{k6} , respectively (Fig. 7). The values of E_a , ΔH^\ddagger and ΔG^\ddagger for the k_5 (k_6) steps are 89.00, 86.90 and 98.92 kJ mol^{-1} (78.85, 72.44 and 99.66 kJ mol^{-1}), respectively (Table II). The total activation energy, the total activation enthalpy and the total activation Gibbs energy change

for the COCl/PCA2 (COCl/PCA3) mechanism are 84.32, 88.31 and 129.12 kJ mol⁻¹ (75.05, 74.88 and 128.82 kJ mol⁻¹), respectively (Table II).

The energy profile for the COOH and COCl mechanisms is shown in Fig. 8. The total activation energies for the COCl/PCA1–3 mechanisms are lower than the COOH/PCA1–3 mechanisms by 156.04, 93.63 and 22.99 kJ mol⁻¹, respectively. Amongst the COCl/PCA1–3 mechanisms, the contribution of the COCl/PCA1 mechanism is higher.

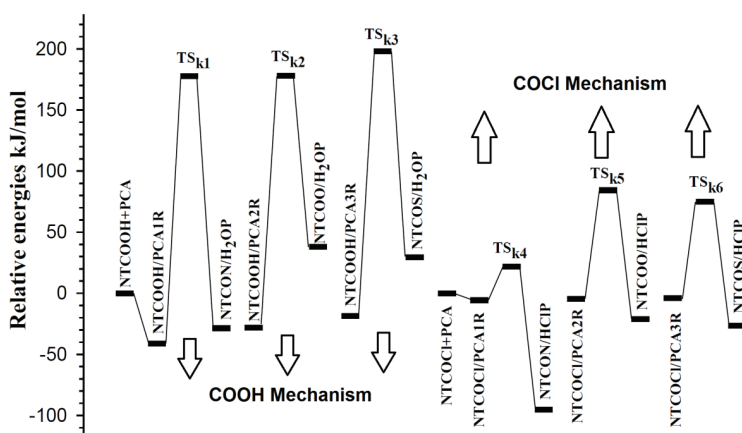


Fig. 8. Energy profile for the COOH and COCl mechanisms.

Both mechanisms (COOH and COCl) are nucleophilic substitution reactions. Generally, these reactions proceed through a tetrahedral intermediate. Thus, a tetrahedral intermediate was designed as input and ultimately a structure was optimized that is similar to the reactant NTCOCl/PCA. This means that a tetrahedral intermediate could not exist, probably due to electronic and steric effects of carbon nanotubes.

CONCLUSIONS

Six possible configurations of non-covalent interaction of the drug penicillamine (PCA) onto NTCOOH and NTCOCl were studied. The binding energies related to NTCOCl are lower than those related to NTCOOH, indicating NTCOOH/PCA configurations are stabilized. The global hardness and HOMO–LUMO energy gap of the NTCOOH/PCA configurations are higher than those of the NTCOCl/PCA configurations, showing the reactivity of penicillamine increases in the presence of NTCOCl and its stability decreases.

Two mechanisms of covalent functionalization of the drug penicillamine onto NTCOOH (COOH mechanism) and NTCOCl (COCl mechanism) were investigated in detail. Each mechanism involves three pathways because penicillamine can bond to NTCOOH or NTCOCl through NH₂, OH and SH groups. The

activation parameters related to the COOH mechanisms are higher than those related to the COCl mechanisms. The lowest activation energy is related to the COCl/PCA1 pathway. In this mechanism, penicillamine is bonded to NTCOCl via NH₂ groups.

SUPPLEMENTARY MATERIAL

XYZ coordinates and absolute energies for all computed structures are available electronically at the pages of journal website: <http://www.shd.org.rs/JSCS/>, or from the corresponding author on request.

Acknowledgement. We thank the Research Center for Animal Development Applied Biology for allocation of computer time.

ИЗВОД

МЕХАНИСТИЧКЕ, ЕНЕРГЕТСКЕ И СТРУКТУРНЕ СТУДИЈЕ ПЕНИЦИЛАМИНОМ ФУНКЦИОНАЛИЗОВАНИХ ЈЕДНОЗИДНИХ УГЉЕНИЧНИХ НАНОЦЕВИ

HOSEIN SHAKI¹, ALI MORSALI², HEIDAR RAISSI³, MOHAMMAD HAKIMI¹ и S. ALI BEYRAMABADI²

¹Department of Chemistry, Payame Noor University, P.O.Box 19395–3697, Tehran, Iran, ²Department of Chemistry & Research Center for Animal Development Applied Biology, Mashhad Branch, Islamic Azad University, Mashhad 917568, Iran и ³Department of Chemistry, University of Birjand, Birjand, Iran

Користећи теорију функционала густине проучавање су могуће нековалентне интеракције и шест механизама ковалентног функционализовања лека пенициламина са функционализованим угљеничним наноцевима (CNT). Проучавани су квантномолекулски описници нековалентних конфигурација. Спецификовано је да је везивање лека пенициламина за функционализоване CNT термодинамички повољно. COOH функционализована CNT (NTCOOH) има већу енергију везивања него COCl функционализована CNT (NTCOCl) и може деловати као повољан систем за доставу лека пенициламина у биолошке и хемијске системе (нековалентно). NTCOOH и NTCOCl могу се везати за NH₂, OH и SH групе пенициламина преко OH (COOH механизам) односно Cl (COCl механизам) група. Енергије активације, промене ентальпије активације и промене Гибсове енергије активације су израчунате и узајамно поређене. Активациони параметри који се односе на COOH механизам су виши од оних који се односе на COCl механизам, те је COCl механизам повољан за ковалентно функционализовање. Ови резултати се могу уопштити и за друге сличне лекове.

(Примљено 18. фебруара, ревидирано 29. маја, прихваћено 6. јуна 2017)

REFERENCES

1. G. D. Pennock, W. S. Dalton, W. R. Roeske, C. P. Appleton, K. Mosley, P. Plezia, T. P. Miller, S. E. Salmon, *J. Natl. Cancer Inst.* **83** (1991) 105
2. C. Lindley, J. S. McCune, T. E. Thomason, D. Lauder, A. Sauls, S. Adkins, W. T. Sawyer, *Cancer Pract.* **7** (1999) 59
3. S. N. Marinković, *J. Serb. Chem. Soc.* **73** (2008) 891
4. U. N. Maiti, W. J. Lee, J. M. Lee, Y. Oh, J. Y. Kim, J. E. Kim, J. Shim, T. H. Han, S. O. Kim, *Adv. Mater.* **26** (2014) 40
5. H. Yaghoubian, H. Karimi-Maleh, M. A. Khalilzadeh, F. Karimi, *J. Serb. Chem. Soc.* **74** (2009) 1443

6. C. Rungnim, U. Arsawang, T. Rungrotmongkol, S. Hannongbua, *Chem. Phys. Lett.* **550** (2012) 99
7. M. Adeli, R. Soleiman, Z. Beiranvand, F. Madani, *Chem. Soc. Rev.* **42** (2013) 5231
8. R. V. Mundra, X. Wu, J. Sauer, J. S. Dordick, R. S. Kane, *Curr. Opin. Biotechnol.* **28** (2014) 25
9. M. Karimi, N. Solati, A. Ghasemi, M. A. Estiar, M. Hashemkhani, P. Kiani, E. Mohamed, A. Saeidi, M. Taheri, P. Avci, *Expert Opin. Drug Delivery* **12** (2015) 1089
10. H. Zhang, L. Hou, X. Jiao, Y. Ji, X. Zhu, H. Li, X. Chen, J. Ren, Y. Xia, Z. Zhang, *Curr. Pharm. Biotechnol.* **14** (2014) 1105
11. S. Unnati, R. Shah, *Int. J. Pharm. Technol.* **3** (2011) 927
12. B. S. Wong, S. L. Yoong, A. Jagusiak, T. Panczyk, H. K. Ho, W. H. Ang, G. Pastorin, *Adv. Drug Delivery Rev.* **65** (2013) 1964
13. Y. Lin, L. F. Allard, Y. P. J. Sun, *Phys. Chem., B* **108** (2004) 3760
14. E. A. Gad, J. H. Al-Fahemi, K. S. Khairou, *J. Comput. Theor. Nanosci.* **11** (2014) 404
15. H. Yahyaei, M. Monajjemi, H. Aghaie, K. Zare, *J. Comput. Theor. Nanosci.* **10** (2013) 2332
16. C. M. Chang, H. L. Tseng, A. de Leon, A. Posada-Amarillas, A. F. Jalbout, *J. Comput. Theor. Nanosci.* **10** (2013) 521
17. S. Rahimi-Razin, V. Haddadi-Asl, M. Salami-Kalajahi, F. Behboodi-Sadabad, H. Roghani-Mamaqani, *Int. J. Chem. Kinet.* **44** (2012) 555
18. M. Prato, K. Kostarelos, A. Bianco, *Acc. Chem. Res.* **41** (2007) 60
19. T. M. Allen, P. R. Cullis, *Science* **303** (2004) 1818
20. D. Tomalia, L. Reyna, S. Svenson, *Biochem. Soc. Trans.* **35** (2007) 61
21. E. Flahaut, in *Carbon Nanotubes for Biomedical Applications*, Springer, Berlin, 2011, p. 211
22. K. Ajima, M. Yudasaka, T. Murakami, A. Maigné, K. Shiba, S. Iijima, *Mol. Pharmaceutics* **2** (2005) 475
23. J. Peisach, W. Blumberg, *Mol. Pharmacol.* **5** (1969) 200
24. A. Camp, *J. Rheumatol.* **7** (1980) 103
25. S. Wadhwa, R. J. Mumper, *Cancer Lett.* **337** (2013) 8
26. A. Khorsand, S. Jamehbozorgi, R. Ghiasi, M. Rezvani, *Phys. E (Amsterdam, Neth.)* **72** (2015) 120
27. Y. B. Zheng, B. Kiraly, T. J. Huang, *Nanomedicine (London, U.K.)* **5** (2010) 1309
28. V. Linko, A. Ora, M. A. Kostiainen, *Trends Biotechnol.* **33** (2015) 586
29. W. Szymański, J. M. Beierle, H. A. Kistemaker, W. A. Velema, B. L. Feringa, *Chem. Rev.* **113** (2013) 6114
30. C. Rungnim, T. Rungrotmongkol, S. Hannongbua, H. Okumura, *J. Mol. Graphics Modell.* **39** (2013) 183
31. A. D. Becke, *Phys. Rev., A* **38** (1988) 3098
32. A. D. Becke, *J. Chem. Phys.* **98** (1993) 5648
33. C. Lee, W. Yang, R. G. Parr, *Phys. Rev. B* **37** (1988) 785
34. Gaussian 09, Revision A.02, Gaussian, Inc., Wallingford CT, 2009
35. S. Hooman Vahidi, A. Morsali, S. A. Beyramabadi, *Comput. Theor. Chem.* **994** (2012) 41
36. A. Akbari, F. Hoseinzade, A. Morsali, S. Ali Beyramabadi, *Inorg. Chim. Acta* **394** (2013) 423
37. A. Morsali, F. Hoseinzade, A. Akbari, S. A. Beyramabadi, R. Ghiasi, *J. Solution Chem.* **42** (2013) 1902
38. S. Mohseni, M. Bakavoli, A. Morsali, *Prog. React. Kinet. Mech.* **39** (2014) 89

39. S. A. Beyramabadi, H. Eshtiagh-Hosseini, M. R. Housaindokht, A. Morsali, *Organometallics* **27** (2007) 72
40. A. Gharib, A. Morsali, S. Beyramabadi, H. Chegini, M. N. Ardabili, *Prog. React. Kinet. Mech.* **39** (2014) 354
41. A. Morsali, *Int. J. Chem. Kinet.* **47** (2015) 73
42. M. N. Ardabili, A. Morsali, S. A. Beyramabadi, H. Chegini, A. Gharib, *Res. Chem. Intermed.* **41** (2015) 5389
43. M. Domínguez, V. G. Machado, L. G. Nandi, M. C. Rezende, P. Silva, *Int. J. Chem. Kinet.* **47** (2015) 803
44. R. Cammi, J. Tomasi, *J. Comput. Chem.* **16** (1995) 1449
45. J. Tomasi, M. Persico, *Chem. Rev.* **94** (1994) 2027
46. J. B. Foresman, AE. Frisch, *Exploring Chemistry with Electronic Structure Methods*, 3rd ed., Gaussian, Inc., Wallingford, CT, 2015
47. S. Dapprich, I. Komáromi, K. S. Byun, K. Morokuma, M. J. Frisch, *J. Mol. Struct.: THEOCHEM* **461** (1999) 1
48. R. G. Parr, L. V. Szentpaly, S. Liu, *J. Am. Chem. Soc.* **121** (1999) 1922
49. Y. Zhao, D. G. Truhlar, *Theor. Chem. Acc.* **120** (2008) 215
50. T. Lin, V. Bajpai, T. Ji, L. Dai, *Aust. J. Chem.* **56** (2003) 635.